Mathematical aspects and simulation of electron-electron scattering in graphene

Giovanni Nastasi*   Vittorio Romano†

Abstract

Some properties of the electron-electron collision operator in graphene are analyzed along with the evaluation of collision rate. Monte Carlo simulations complete the study and highlight the non negligible role of the electron-electron scattering for an accurate evaluation of the currents and, as a consequence, of the characteristic curves.

Keywords Graphene; charge transport; electron-electron scattering; Direct Simulation Monte Carlo

1   Introduction

Some mathematical and computational issues arising when the electron-electron scattering is included in the analysis of charge transport in graphene are investigated. The electron-phonon interactions are more effective but electron-electron scattering cannot be neglected in some regimes. The appropriate expression for the electron-electron scattering rate is still matter of debate (see for example [1, 2, 3, 5, 6, 7, 8, 9, 10]); however, some mathematical considerations can be made only on the basis of the general properties, such conservation of energy and crystal momentum during the collision when umklapp effects are neglected. These can be relevant but usually at low temperatures. Here the analysis is performed having in mind room temperature.

We have found the general form of the collisional invariants and the kernel of the electron-electron scattering. The latter is constituted by a family of distribution functions which generalize the Fermi-Dirac one and belong to a five-dimensional manifold. If both electron-phonon and electron-electron scatterings are taken into account, the equilibria lie on a two-dimensional sub-manifold. It is interesting to stress that the results are analogous to that obtained in the relativistic case [11]. This is not surprising since the electron

---

*Department of Mathematics and Computer Science, University of Catania, Viale Andrea Doria 6, 95125 Catania, Italy (`giovanni.nastasi@unict.it`).

†Department of Mathematics and Computer Science, University of Catania, Viale Andrea Doria 6, 95125 Catania, Italy (`romano@dmi.unict.it`).

inside graphene move like massless fermions for wave-vectors around the Dirac points [12]. However, our derivation requires less regularity than that assumed in [11] and does not use concepts of Special Relativity.

To complete the investigation, an estimation of the electron-electron scattering rate is given and employed in a DSMC code based on the approach proposed in [13] which allows an efficient and accurate inclusion of the Pauli exclusion principle. Simulations of charge transport in suspended monolayer graphene indicate a variation in the average electron velocity of about 13 %, at least in the considered cases, giving a confirmation of the importance of the electron-electron scattering according to [3].

The plan of the paper is as follows. In Sec. 2 the semiclassical Boltzmann equation is introduced and in particular the main features of the electron-electron scattering are recalled. Sec. 3 is devoted to the analysis of the properties of the electron-electron collision operator in graphene such as the collision invariants and the kernel. In Sec.s 4 and 5 the electron-electron scattering rate is evaluated in the intra-band case and in the inter-band case, respectively. The last section contains the results of the Monte Carlo simulations in order to assess the importance of the electron-electron scattering with respect to the electron-phonon ones.

2 Semiclassical transport and electron-electron scattering

Electrons moving inside a graphene sheet are located in the wave-vector space mainly around the Dirac points (here considered as equivalent). With a good approximation, the energy bands can be assumed linear in the modulus of the wave-vector $\mathbf{k}$, measured with respect to the Dirac point $\mathbf{k}_l$, with a zero gap between the valence and the conduction bands. We, therefore, assume that the energy band ε with respect to the Dirac energy ε_D is given by

$$\varepsilon(\mathbf{k}) = \alpha \hbar v_F |\mathbf{k} - \mathbf{k}_l|.$$

with $\alpha = 1$ in the conduction band and $\alpha = -1$ in the valence band, and extend such a dispersion relation to any $\mathbf{k} \in \mathbb{R}^2$.

The electron velocity is given by

$$\mathbf{v}_\alpha = \frac{1}{\hbar} \nabla_{\mathbf{k}} \varepsilon_\alpha,$$

Observe that the energy band is negative in the valence band.

The semiclassical Boltzmann equations for the distributions (occupation numbers) $f_\alpha(\mathbf{r}, \mathbf{k}, t)$, at the position $\mathbf{r}$, wave-vector $\mathbf{k}$ and time t, of electrons in the conduction

band ($\alpha = 1$) and in the valence band ($\alpha = -1$) reads (see [2])

$$
\frac{\partial f_\alpha(\mathbf{k})}{\partial t} + \mathbf{v}_\alpha \cdot \nabla_{\mathbf{r}} f_\alpha(\mathbf{k}) - \frac{e}{\hbar} \mathbf{E} \cdot \nabla_{\mathbf{k}} f_\alpha(\mathbf{k})
$$
$$
= \sum_{\eta, \alpha', \mathbf{k}'} \left[S^\eta_{\alpha', \alpha}(\mathbf{k}', \mathbf{k}) f_{\alpha'}(\mathbf{k}')(1 - f_\alpha(\mathbf{k})) - S^\eta_{\alpha, \alpha'}(\mathbf{k}, \mathbf{k}') f_\alpha(\mathbf{k})(1 - f_{\alpha'}(\mathbf{k}')) \right]
$$
$$
+ \sum_{\alpha', \mathbf{k}_*, \mathbf{k}', \mathbf{k}'_2} \left[S_{ee}(\mathbf{k}', \mathbf{k}'_*, \mathbf{k}, \mathbf{k}_*) f_\alpha(\mathbf{k}') f_{\alpha'}(\mathbf{k}'_*)(1 - f_\alpha(\mathbf{k}))(1 - f_{\alpha'}(\mathbf{k}_*)) \right.
$$
$$
\left. - S_{ee}(\mathbf{k}, \mathbf{k}_*, \mathbf{k}', \mathbf{k}'_*) f_\alpha(\mathbf{k}) f_{\alpha'}(\mathbf{k}_*)(1 - f_\alpha(\mathbf{k}'))(1 - f_{\alpha'}(\mathbf{k}'_*)) \right], \tag{1}
$$

where we have explicitly written only the dependence of f_α on $\mathbf{k}$ for the sake of simplicity. Eq.s (1) include both the electron-phonon and the electron-electron scatterings, even if for low densities the second one is usually considered negligible.

The $S^\eta_{\alpha', \alpha}$'s are the transition rate due to the scattering of electrons with phonons in the η branch, where η ranges in the set LA (longitudinal acoustic), TA (transversal acoustic), LO (longitudinal optical), TO (transversal optical) and K phonons. Indeed there exist also the flexural mode, the so-called Z-phonons, but they do not interact with electrons and play a relevant role only for the determination of the crystal temperature [14]. S_{ee} is the electron-electron transition rate. Umklapp effects will be neglected.

The transition rate due to the scattering of electrons with phonons in the νth branch has the form

$$
S_{s', s}(\mathbf{k}', \mathbf{k}) = \sum_\nu \left| G^{(\nu)}_{s', s}(\mathbf{k}', \mathbf{k}) \right|^2 \left[\left(n^{(\nu)}_{\mathbf{q}} + 1 \right) \delta \left(\varepsilon_s(\mathbf{k}) - \varepsilon_{s'}(\mathbf{k}') + \hbar \omega^{(\nu)}_{\mathbf{q}} \right) \right.
$$
$$
\left. + n^{(\nu)}_{\mathbf{q}} \delta \left(\varepsilon_s(\mathbf{k}) - \varepsilon_{s'}(\mathbf{k}') - \hbar \omega^{(\nu)}_{\mathbf{q}} \right) \right]. \tag{2}
$$

$\left| G^{(\nu)}_{s', s}(\mathbf{k}', \mathbf{k}) \right|$ is the matrix element, the symbol δ denotes the Dirac distribution, $\omega^{(\nu)}_{\mathbf{q}}$ is the the νth phonon frequency, $n^{(\nu)}_{\mathbf{q}}$ is the Bose-Einstein distribution for the phonon of type ν

$$
n^{(\nu)}_{\mathbf{q}} = \frac{1}{e^{\hbar \omega^{(\nu)}_{\mathbf{q}} / k_B T} - 1},
$$

k_B is the Boltzmann constant and T is the graphene lattice temperature which, in this article, will be kept constant. When, for a phonon ν_*, $\hbar \omega^{(\nu_*)}_{\mathbf{q}} \ll k_B T$, then the scattering with the phonon ν_* can be assumed elastic. In this case, we eliminate in Eq. (2) the term $\hbar \omega^{(\nu_*)}_{\mathbf{q}}$ inside the delta distribution and we use the approximation $n^{(\nu_*)}_{\mathbf{q}} + 1 \approx n^{(\nu_*)}_{\mathbf{q}}$. For acoustic phonons, usually one considers the elastic approximation, and

$$
2 n^{(ac)}_{\mathbf{q}} \left| G^{(ac)}(\mathbf{k}', \mathbf{k}) \right|^2 = \frac{1}{(2\pi)^2} \frac{\pi D^2_{ac} k_B T}{2 \hbar \sigma_m v^2_p} (1 + \cos \vartheta_{\mathbf{k}, \mathbf{k}'}), \tag{3}
$$

where D_{ac} is the acoustic phonon coupling constant, v_p is the sound speed in graphene, σ_m the graphene areal density, and $\vartheta_{\mathbf{k}, \mathbf{k}'}$ is the convex angle between $\mathbf{k}$ and $\mathbf{k}'$.

There are three relevant optical phonon scatterings: the longitudinal optical (LO), the transversal optical (TO) and the K phonons. The matrix elements are

$$\left|G^{(LO)}(\mathbf{k}',\mathbf{k})\right|^2 + \left|G^{(TO)}(\mathbf{k}',\mathbf{k})\right|^2 = \frac{2}{(2\pi)^2}\frac{\pi D_O^2}{\sigma_m \omega_O} \tag{4}$$

$$\left|G^{(K)}(\mathbf{k}',\mathbf{k})\right|^2 = \frac{1}{(2\pi)^2}\frac{2\pi D_K^2}{\sigma_m \omega_K}(1 - \cos\vartheta_{\mathbf{k},\mathbf{k}'}), \tag{5}$$

where D_O is the optical phonon coupling constant, ω_O the optical phonon frequency, D_K is the K-phonon coupling constant and ω_K the K-phonon frequency. Physical parameters for the collision terms are summarized in Table 1.

v_F	10^8 cm/s	v_p	2×10^6 cm/s
σ_m	7.6×10^{-8} g/cm^2	D_{ac}	6.8 eV
$\hbar\omega_O$	164.6 meV	D_O	10^9 eV/cm
$\hbar\omega_K$	124 meV	D_K	3.5×10^8 eV/cm

Table 1: Physical parameters for the collision terms.

$S_{ee}(\mathbf{k}_1, \mathbf{k}_2, \mathbf{k}_1', \mathbf{k}_2')$ represents the probability of transition, for unit time, from the joint state $(\mathbf{k}_1, \mathbf{k}_2)$ to the joint state $(\mathbf{k}_1', \mathbf{k}_2')$. In this paper only normal scatterings are considered and umklapp processes are neglected.

According to the Fermi golden rule [3] (for similar approaches in other contexts see [15, 16], S_{ee} is given by

$$S_{ee}(\mathbf{k}_1, \mathbf{k}_2, \mathbf{k}_1', \mathbf{k}_2') = \frac{2\pi}{\hbar}|M|^2\delta(\varepsilon(\mathbf{k}_1')) + \varepsilon(\mathbf{k}_2')) - \varepsilon(\mathbf{k}_1)) - \varepsilon(\mathbf{k}_2))).$$

M is the matrix interaction, whose generic element is given by

$$|M|^2 = \frac{1}{2}\left[|V(q)|^2 + |V(q')|^2 - V(q)V(q')\right],$$

where $V(q)$ is the Coulomb potential between pairs of electrons having momenta $\mathbf{k}_1$ and $\mathbf{k}_1'$

$$V(q) = \frac{2\pi e^2}{\epsilon(q)qA}\frac{1 + \cos(\phi_{\mathbf{k}_1,\mathbf{k}_1'})}{2}\frac{1 + \cos(\phi_{\mathbf{k}_2,\mathbf{k}_2'})}{2},$$

with $q = |\mathbf{k}_1 - \mathbf{k}_1'|$. Similarly

$$V(q') = \frac{2\pi e^2}{\epsilon(q')q'A}\frac{1 + \cos(\phi_{\mathbf{k}_1,\mathbf{k}_2'})}{2}\frac{1 + \cos(\phi_{\mathbf{k}_2,\mathbf{k}_1'})}{2},$$

with $q' = |\mathbf{k}_1 - \mathbf{k}_2'|$.

In the above expressions, $\phi_{\mathbf{k},\mathbf{k}'}$ denotes the angle between $\mathbf{k}$ and $\mathbf{k}'$. More sophisticated models are present in the literature. The interested reader is referred to [5, 6, 7].

In the *random-phase approximation* (valid when $n \geq 10^{12} cm^{-2}$), the dielectric function $\epsilon(q)$ is given by (see [8])

$$\epsilon(q) = 1 + v_c(q)\Pi(q),$$

where $v_c(q) = 2\pi e^2/\kappa q$, κ being the *background lattice dielectric constant* which satisfies

$$r_s = \frac{e^2}{\kappa\gamma}\sqrt{\frac{4}{g_s g_v}}. \tag{6}$$

Here, $\gamma = \hbar v_F$, g_s and g_v are the spin and valley degenerations respectively; r_s is a constant representing the adimensional *Wigner-Seitz radius*; $\Pi(q) = D(E_F)\widetilde{\Pi}(q)$, with ε_F the Fermi energy and D is the density of states given by

$$D(\varepsilon) = \frac{g_v g_s |\varepsilon|}{2\pi\gamma^2}. \tag{7}$$

The function $\widetilde{\Pi}(q)$ is usually decomposed as $\widetilde{\Pi}(q) = \widetilde{\Pi}^-(q) + \widetilde{\Pi}^+(q)$ with

$$\widetilde{\Pi}^-(q) = \frac{\pi q}{8k_F}$$

$$\widetilde{\Pi}^+(q) = \begin{cases} 1 - \dfrac{\pi q}{8k_F} & \text{if} \quad q < 2k_F \\[2mm] 1 - \dfrac{\sqrt{q^2 - 4k_F^2}}{2q} - \dfrac{q}{4k_F}\arcsin\left(\dfrac{2k_F}{q}\right) & \text{otherwise} \end{cases},$$

where $k_F = \sqrt{4\pi n/g_s g_v}$ is the Fermi momentum which satisfies $\varepsilon_F = \gamma k_F$ and n is the electron density. More details can be found in [1, 9].

3 Properties of the electron-electron collision operator in graphene

In any binary collision the conservation laws of crystal momentum and energy have to be satisfied in a normal scattering [17]

$$\hbar\mathbf{k} + \hbar\mathbf{k}_* = \hbar\mathbf{k}' + \hbar\mathbf{k}'_*, \tag{8}$$

$$\hbar v_F|\mathbf{k} - \mathbf{k}_l| + \hbar v_F|\mathbf{k}_* - \mathbf{k}_l| = \hbar v_F|\mathbf{k}' - \mathbf{k}_l| + \hbar v_F|\mathbf{k}'_* - \mathbf{k}_l| \tag{9}$$

$\mathbf{k}$ and $\mathbf{k}_*$ are the crystal momenta of the incoming particles, $\mathbf{k}'$ and $\mathbf{k}'_*$ are the crystal momenta of the outgoing particles. Indeed, in general the crystal momentum is not the momentum of the electron but it is customary in solid state physics to assume the approximation of the conservation of the crystal momentum.

After the translation $\mathbf{k} - \mathbf{k}_l \to \mathbf{k}$ the previous conservation laws read (note that the conservation of momentum is invariant under translation)

$$\mathbf{k} + \mathbf{k}_* = \mathbf{k}' + \mathbf{k}'_*, \tag{10}$$

$$|\mathbf{k}| + |\mathbf{k}_*| = |\mathbf{k}'| + |\mathbf{k}'_*|. \tag{11}$$

Definition 1. *A function φ is said a collisional invariant if it satisfies the condition*

$$\varphi + \varphi_* = \varphi' + \varphi'_*, \tag{12}$$

where the following shorthand notation has been used: $\varphi := \varphi(\mathbf{k})$, $\varphi_* := \varphi(\mathbf{k}_*)$, $\varphi' := \varphi(\mathbf{k}')$, $\varphi'_* := \varphi(\mathbf{k}'_*)$.

We want to determine the most general form of the collision invariant for the electron-electron scattering (hereafter EES). To this aim we introduce the following two lemmas.

Lemma 1. *Let E_n be a n-dimensional Euclidean real vector space, endowed with the canonical scalar product and let $f(\mathbf{x})$ be a real function on E_n which is continuous al least in a point and satisfies*

$$f(\mathbf{x}) + f(\mathbf{x}_1) = f(\mathbf{x} + \mathbf{x}_1) \tag{13}$$

for each $\mathbf{x}, \mathbf{x}_1 \in E_n$. Then $f(\mathbf{x}) = \mathbf{A} \cdot \mathbf{x}$ where $\mathbf{A}$ is a constant vector.

The proof is standard. The interested reader can see for example [18].

Lemma 2. *Let $f : \mathbb{R}^n \to \mathbb{R}$ be a differentiable function which is homogeneous of degree one (that is $f(\lambda \mathbf{x}) = \lambda f(\mathbf{x}) \ \forall \ \lambda \in \mathbb{R}$). Then f is linear.*

Proof. The homogeneity means

$$f(\lambda x_1, \ldots, \lambda x_n) = \lambda f(x_1, \ldots, x_n).$$

and by taking the derivatives with respect to λ of both sides one has

$$f(\mathbf{x}) = \nabla_\mathbf{x} f(\lambda \mathbf{x}) \cdot \mathbf{x}.$$

Passing to the limit as $\lambda \to 0$, one gets

$$f(\mathbf{x}) = \nabla_\mathbf{x} f\big|_\mathbf{0} \cdot \mathbf{x}$$

and therefore, being $\nabla_\mathbf{x} f\big|_\mathbf{0}$ a constant vector, it follows that $f(\mathbf{x})$ is linear. $\square$

Now we are in the position to establish the general form of the collision invariants.

Theorem 1. *Let $\varphi(\mathbf{k})$ a continuous function whose odd part is differentiable. $\varphi(\mathbf{k})$ is a collisional invariant if and only if*

$$\varphi(\mathbf{k}) = a + \mathbf{b} \cdot \mathbf{k} + c|\mathbf{k}| \tag{14}$$

for arbitrary $a, c \in \mathbb{R}$ and arbitrary $\mathbf{b} \in \mathbb{R}^2$.

Proof. The equation (12) implies that $\varphi + \varphi_*$ takes the same values for all the pairs of vectors $(\mathbf{k}, \mathbf{k}_*)$ that satisfy the conservation laws (8), (9), that is $\varphi + \varphi_*$ is constant whenever $\mathbf{k} + \mathbf{k}_*$ and $|\mathbf{k}| + |\mathbf{k}_*|$ are constant. This means that $\varphi + \varphi_*$ is a function which depends only on such quantities, in other words

$$\varphi(\mathbf{k}) + \varphi(\mathbf{k}_*) = \Phi(|\mathbf{k}| + |\mathbf{k}_*|, \mathbf{k} + \mathbf{k}_*) \tag{15}$$

for a suitable function Φ. Let us introduce

$$\varphi_\pm(\mathbf{k}) = \varphi(\mathbf{k}) \pm \varphi(-\mathbf{k}),$$

$$\Phi_\pm(|\mathbf{k}| + |\mathbf{k}_*|, \mathbf{k} + \mathbf{k}_*) = \Phi(|\mathbf{k}| + |\mathbf{k}_*|, \mathbf{k} + \mathbf{k}_*) \pm \Phi(|\mathbf{k}| + |\mathbf{k}_*|, -\mathbf{k} - \mathbf{k}_*).$$

After the substitution $(\mathbf{k}, \mathbf{k}_*) \to (-\mathbf{k}, -\mathbf{k}_*)$, relation (15) becomes

$$\varphi(-\mathbf{k}) + \varphi(-\mathbf{k}_*) = \Phi(|\mathbf{k}| + |\mathbf{k}_*|, -\mathbf{k} - \mathbf{k}_*). \tag{16}$$

(15) + (16) $\Rightarrow \varphi(\mathbf{k}) + \varphi(-\mathbf{k}) + \varphi(\mathbf{k}_*) + \varphi(-\mathbf{k}_*) = \Phi(|\mathbf{k}| + |\mathbf{k}_*|, \mathbf{k} + \mathbf{k}_*) + \Phi(|\mathbf{k}| + |\mathbf{k}_*|, -\mathbf{k} - \mathbf{k}_*).$
(15) - (16) $\Rightarrow \varphi(\mathbf{k}) - \varphi(-\mathbf{k}) + \varphi(\mathbf{k}_*) - \varphi(-\mathbf{k}_*) = \Phi(|\mathbf{k}| + |\mathbf{k}_*|, \mathbf{k} + \mathbf{k}_*) - \Phi(|\mathbf{k}| + |\mathbf{k}_*|, -\mathbf{k} - \mathbf{k}_*).$
In a compact form one has

$$\varphi_\pm(\mathbf{k}) + \varphi_\pm(\mathbf{k}_*) = \Phi_\pm(|\mathbf{k}| + |\mathbf{k}_*|, \mathbf{k} + \mathbf{k}_*). \tag{17}$$

Observe that

$$\varphi_\pm(-\mathbf{k}) = \pm\varphi_\pm(\mathbf{k}).$$

If we take $\mathbf{k}_* = -\mathbf{k}$ then

$$\varphi_+(\mathbf{k}) + \varphi_+(-\mathbf{k}) = 2\varphi_+(\mathbf{k}) = \Phi_+(2|\mathbf{k}|, \mathbf{0}). \tag{18}$$

As a consequence φ_+ depends only on $|\mathbf{k}|$, that is $\varphi_+(\mathbf{k}) = \psi(|\mathbf{k}|)$. This implies, on account of (17), that Φ_+ depends only on $|\mathbf{k}| + |\mathbf{k}_*|$ because no function (apart from the constant case) of $\mathbf{k} + \mathbf{k}_*$ can be built from $|\mathbf{k}|$ and $|\mathbf{k}_*|$. In fact, by absurd, let us suppose that $f(\mathbf{k} + \mathbf{k}_*) = g(|\mathbf{k}|, |\mathbf{k}_*|)$ then setting $\mathbf{k}_* = \mathbf{0}$, one has $f(\mathbf{k}) = h(|\mathbf{k}|)$. Therefore $f(\mathbf{k} + \mathbf{k}_*) = h(|\mathbf{k} + \mathbf{k}_*|)$, that is $h(\sqrt{|\mathbf{k}|^2 + |\mathbf{k}_*|^2 + 2\mathbf{k} \cdot \mathbf{k}_*}) = g(|\mathbf{k}|, |\mathbf{k}_*|)$. By choosing $\mathbf{k} \cdot \mathbf{k}_* = 0$, one gets $h(\sqrt{|\mathbf{k}|^2 + |\mathbf{k}_*|^2}) = g(|\mathbf{k}|, |\mathbf{k}_*|)$; instead by choosing $\mathbf{k}_* = \mathbf{k}$, one finds $h(|\mathbf{k}| + |\mathbf{k}_*|) = g(|\mathbf{k}|, |\mathbf{k}_*|)$. The two expressions of g are compatible only in the cases $\mathbf{k} = 0$ or $\mathbf{k}_* = 0$. This implies that h must be constant leading to a contradiction.

Now from (17) it is possible to write

$$\psi(|\mathbf{k}|) + \psi(|\mathbf{k}_*|) = \Phi_+(|\mathbf{k}| + |\mathbf{k}_*|).$$

Setting $\mathbf{k}_* = \mathbf{0}$ we find

$$\psi(|\mathbf{k}|) + \psi(0) = \Phi_+(|\mathbf{k}|)$$

and therefore

$$\psi(|\mathbf{k}| + |\mathbf{k}_*|) + \psi(0) = \Phi_+(|\mathbf{k}| + |\mathbf{k}_*|)$$

7

wherefrom
$$\psi(|\mathbf{k}|) + \psi(|\mathbf{k}_*|) = \psi(|\mathbf{k}| + |\mathbf{k}_*|) + \psi(0).$$

Summing up to both sides the quantity $-2\psi(0)$ one get

$$\psi(|\mathbf{k}|) - \psi(0) + \psi(|\mathbf{k}_*|) - \psi(0) = \psi(|\mathbf{k}| + |\mathbf{k}_*|) - \psi(0).$$

Setting $f(x) = \psi(x) - \psi(0)$ one has

$$f(|\mathbf{k}|) + f(|\mathbf{k}_*|) = f(|\mathbf{k}| + |\mathbf{k}_*|).$$

Applying Lemma 1 in the one dimensional case, we can conclude that $f(|\mathbf{k}|) = 2c|\mathbf{k}|$. As a consequence

$$\varphi_+(|\mathbf{k}|) = \psi(|\mathbf{k}|) = f(|\mathbf{k}|) + \psi(0) = 2c|\mathbf{k}| + 2a,$$

where $\psi(0) = 2a$ is a constant.

Let us consider the equation (17) for φ_- and observe that

$$(\mathbf{k} + \mathbf{k}_*)^2 = |\mathbf{k}|^2 + |\mathbf{k}_*|^2 + 2\mathbf{k} \cdot \mathbf{k}_* = (|\mathbf{k}| + |\mathbf{k}_*|)^2 + 2(\mathbf{k} \cdot \mathbf{k}_* - |\mathbf{k}||\mathbf{k}_*|).$$

Then Φ_- depends only on $\mathbf{k} + \mathbf{k}_*$ if $\mathbf{k} \cdot \mathbf{k}_* = |\mathbf{k}||\mathbf{k}_*|$. In this way one has

$$\varphi_-(\mathbf{k}) + \varphi_-(\mathbf{k}_*) = h(\mathbf{k} + \mathbf{k}_*).$$

If we choose $\mathbf{k}_* = \mathbf{0}$ and observe that on account of (3) one has $\varphi_-(\mathbf{0}) = 0$, we get

$$\varphi_-(\mathbf{k}) = h(\mathbf{k})$$

wherefrom

$$\varphi_-(\mathbf{k}) + \varphi_-(\mathbf{k}_*) = \varphi_-(\mathbf{k} + \mathbf{k}_*). \tag{19}$$

under the condition $\mathbf{k} \cdot \mathbf{k}_* = |\mathbf{k}||\mathbf{k}_*|$.

If we choose $\mathbf{k}_* = \mathbf{k}$ one has

$$2\varphi_-(\mathbf{k}) = \varphi_-(2\mathbf{k}).$$

We want to prove that

$$n\varphi_-(\mathbf{k}) = \varphi_-(n\mathbf{k}), \forall n \in \mathbb{N}$$

by induction. In fact, the formula is true for $n = 0, 1, 2$. Let us suppose that $(n-1)\varphi_-(\mathbf{k}) = \varphi_-((n-1)\mathbf{k})$ holds true and evaluate

$$n\varphi_-(\mathbf{k}) = (n-1)\varphi_-(\mathbf{k}) + \varphi_-(\mathbf{k}) = \varphi_-((n-1)\mathbf{k}) + \varphi_-(\mathbf{k}).$$

Observing that

$$(n-1)\mathbf{k} \cdot \mathbf{k} = (n-1)|\mathbf{k}|^2 = |(n-1)\mathbf{k}||\mathbf{k}|,$$

by (19) we find

$$n\varphi_-(\mathbf{k}) = \varphi_-((n-1+1)\mathbf{k}) = \varphi_-(n\mathbf{k}).$$

Let us consider now for each $n, m \in \mathbb{N}$

$$m\varphi_- \left(\frac{n}{m}\mathbf{k} \right) = \varphi_-(m\frac{n}{m}\mathbf{k}) = \varphi_-(n\mathbf{k}) = n\varphi_-(\mathbf{k}),$$

which implies

$$\varphi_-(q\mathbf{k}) = q\varphi_-(\mathbf{k}), \qquad \forall q \in \mathbb{Q}^+$$

The functions $\varphi_-(q\mathbf{k})$ and $q\varphi_-(\mathbf{k})$ are continuous and have the same values for each $q \in \mathbb{Q}$. By a density argument, $\varphi_-(\alpha\mathbf{k}) = \alpha\varphi_-(\mathbf{k})$ for each $\alpha \in \mathbb{R}$, that is φ_- is a homogeneous function in $\mathbb{R}$.

By virtue of Lemma 2 and the differentiability of φ_-, it follows that φ_- is linear and therefore by Lemma 1 we have

$$\varphi_-(\mathbf{k}) = 2\mathbf{b} \cdot \mathbf{k}, \tag{20}$$

for a suitable constant vector $\mathbf{b}$. Since $\varphi = (\varphi_+ + \varphi_-)/2$, the proof is complete. $\qquad\square$

Remark 1. *Going back to the frame centered in Γ, the collisional invariants take the form*

$$\varphi(\mathbf{k}) = a + \mathbf{b} \cdot (\mathbf{k} - \mathbf{k}_l) + c|\mathbf{k} - \mathbf{k}_l| \tag{21}$$

or equivalently

$$\varphi(\mathbf{k}) = a + \mathbf{b} \cdot \mathbf{k} + c|\mathbf{k} - \mathbf{k}_l|. \tag{22}$$

Remark 2. *The expression (14) is formally the same as that found in the relativistic case (see [11] equation (2.56) for particles having zero mass). However, some crucial differences are present. The proof we propose requires only the differentiability of the odd part of the collisional invariant while the proof in [11] is based on the assumption that φ is C^2 which is not true in the case under investigation.*

Our results can be cast in the form expressed by equation (2.56) in [11] by replacing the velocity of light c with the Fermi velocity. It is clear that using Lorentz transformations with v_F instead of c has not a physical rationale because it should mean that the electron velocity inside graphene is invariant with respect to inertial observers. To our knowledge there is no experimental evidence of that.

Before studying the kernel of the electron-electron collision operator, we recall the following symmetry properties that can be directly verified from the expression of S_{ee}:

$$S_{ee}(\mathbf{k}_1, \mathbf{k}_2, \mathbf{k}_1', \mathbf{k}_2') = S_{ee}(\mathbf{k}_2, \mathbf{k}_2, \mathbf{k}_1', \mathbf{k}_2') = S_{ee}(\mathbf{k}_1', \mathbf{k}_2', \mathbf{k}_1, \mathbf{k}_2). \tag{23}$$

Corollary 1. *The kernel of the electron-electron collision operator is given by the function of the form*

$$f(\mathbf{k}) = \frac{1}{1 + \exp\left(a + \mathbf{b} \cdot \mathbf{k} + c|\mathbf{k} - \mathbf{k}_l|\right)} \tag{24}$$

with $a, c \in \mathbb{R}$, $\mathbf{b} \in \mathbb{R}^2$.

Proof. By standard arguments (see for example [19, 20]) one can prove that for any function $g(\mathbf{k})$ regular enough the following relation holds

$$
\begin{aligned}
\int_{\mathbb{R}^2} Q_{ee}(f)g(\mathbf{k})d\mathbf{k} = \int & \frac{\sigma_{ee}(\mathbf{k}, \mathbf{k}_*, \mathbf{k}', \mathbf{k}'_*)}{4}\delta\left(\varepsilon(\mathbf{k}) + \varepsilon(\mathbf{k}_*) - \varepsilon(\mathbf{k}') - \varepsilon(\mathbf{k}'_*)\right) \\
& \times \left(f(\mathbf{k}')f(\mathbf{k}'_*)(1 - f(\mathbf{k}))(1 - f(\mathbf{k}_*)) - f(\mathbf{k})f(\mathbf{k}_*)(1 - f(\mathbf{k}'))(1 - f(\mathbf{k}'_*))\right) \\
& \times \left(g(\mathbf{k}) + g(\mathbf{k}_*) - g(\mathbf{k}') - g(\mathbf{k}'_*)\right) d\mathbf{k}d\mathbf{k}_*d\mathbf{k}'d\mathbf{k}'_*.
\end{aligned} \tag{25}
$$

With the choice

$$
g(\mathbf{k}) = H(f(\mathbf{k})) = \log\frac{f(\mathbf{k})}{1 - f(\mathbf{k})}
$$

it is easy to verify that

$$
\int_{\mathbb{R}^2} Q_{ee}(f)\log\frac{f(\mathbf{k})}{1 - f(\mathbf{k})}d\mathbf{k} \leq 0
$$

and

$$
\int_{\mathbb{R}^2} Q_{ee}(f)\log\frac{f(\mathbf{k})}{1 - f(\mathbf{k})}d\mathbf{k} = 0
$$

if and only if

$$
H(f(\mathbf{k})) + H(f(\mathbf{k}')) = H(f(\mathbf{k}_1)) + H(f(\mathbf{k}'_1))
$$

provided the relations (8)-(9) are satisfied. Therefore, $H(f(\mathbf{k}))$ must be a collisional invariant. On account of the previous theorem

$$
H(f(\mathbf{k})) = a + \mathbf{b} \cdot \mathbf{k} + c|\mathbf{k} - \mathbf{k}_l|,
$$

with $a, c \in \mathbb{R}$, $\mathbf{b} \in \mathbb{R}^2$ arbitrary, wherefrom the expression (24) is obtained. $\qquad\square$

Remark 3. *If we set $a = -\dfrac{\varepsilon_F}{k_B T}$, $\mathbf{b} = \mathbf{0}$ and $c = \pm\dfrac{\hbar v_F}{k_B T}$, where T is the crystal temperature, ε_F is the Fermi energy and k_B is the Boltzmann constant, the standard Fermi-Dirac distribution*

$$
f(\mathbf{k}) = \frac{1}{1 + \exp\left(\dfrac{\varepsilon(|\mathbf{k} - \mathbf{k}_l|) - \varepsilon_F}{k_B T}\right)}, \tag{26}
$$

is recovered, the case of positive and negative sign holding in the conduction and valence band respectively.

Remark 4. *By setting $g(\mathbf{k}) = 1$ from (25) one has the charge conservation (in the unipolar case)*

$$
\int_{\mathbb{R}^2} Q_{ee}(f)d\mathbf{k} = 0,
$$

by setting $g(\mathbf{k}) = \mathbf{k}$ from (25) one has the conservation of the crystal momentum

$$
\int_{\mathbb{R}^2} \mathbf{k}\, Q_{ee}(f)d\mathbf{k} = \mathbf{0},
$$

10

while by setting $g(\mathbf{k}) = \varepsilon(\mathbf{k})$ *from (25) one has the energy conservation*

$$\int_{\mathbb{R}^2} \varepsilon(\mathbf{k}) \, Q_{ee}(f) d\mathbf{k} = 0.$$

Remark 5. *For the electron-phonon scattering by following [21, 19], it is possible to see that the collisional invariants are functions of the type*

$$\varphi(\mathbf{k}) = a + c|\mathbf{k} - \mathbf{k}_l|.$$

and the kernel is spanned by the functions of the form

$$f(\mathbf{k}) = \frac{1}{1 + \exp\left(a + c|\mathbf{k} - \mathbf{k}_l|\right)}. \tag{27}$$

4 Electron-electron scattering rate: the intra-band case

Now we want to address the importance of the electron-electron scattering by Monte Carlo simulations. Other approaches can be used but the complexity of the electron electron collision term makes direct simulations, e.g. based on WENO scheme [22] or Discontinuous Galerkin methods [23], a daunting computational task, unless drastic simplifications are introduced [24, 25]. We will adopt the Monte Carlo scheme presented in [13] which allows a correct inclusion of the Pauli exclusion principle. The details are omitted, the interested reader is referred to reference [13, 26, 14]. Both the intra-band and the inter-band cases will be tackled.

First we consider intra-band scattering.

The scattering rate due to the electron-electron interaction is given by

$$\lambda_{ee}(\mathbf{k}_1) = \sum_{\mathbf{k}_2} f(\mathbf{k}_2) \sum_{\mathbf{k}_1', \mathbf{k}_2'} s_{ee}(\mathbf{k}_1, \mathbf{k}_2, \mathbf{k}_1', \mathbf{k}_2').$$

under the conditions of momentum and energy conservation

$$\mathbf{k}_1 + \mathbf{k}_2 = \mathbf{k}_1' + \mathbf{k}_2', \tag{28}$$

$$|\mathbf{k}_1| + |\mathbf{k}_2| = |\mathbf{k}_1'| + |\mathbf{k}_2'|, \tag{29}$$

with $\mathbf{k}_1$, $\mathbf{k}_2$ states before the scattering and $\mathbf{k}_1'$, $\mathbf{k}_2'$ states after the collision.

The previous relations imply that, given the initial states, the final ones must belong to an ellipse Γ (see Fig. 1). Note that this is true both in the conduction and in the valence band.

If we denote by a, b e c the length of the major, minor and focal semi-axis, assigned $\mathbf{k}_1$ and $\mathbf{k}_2$, one has

$$|\mathbf{k}_1| + |\mathbf{k}_2| = 2a.$$

Moreover, the parallelogram rule gives

$$|\mathbf{k}_1 + \mathbf{k}_2| = 2c$$

and from the relation $a^2 = b^2 + c^2$ one gets b.

Under the above considerations,

$$\lambda_{ee}(\mathbf{k}_1) = \sum_{\mathbf{k}_2} f(\mathbf{k}_2) \sum_{\mathbf{k}_1', \mathbf{k}_2'} \frac{2\pi}{\hbar} |M|^2 \delta(\varepsilon(\mathbf{k}_1') + \varepsilon(\mathbf{k}_2') - \varepsilon(\mathbf{k}_1) - \varepsilon(\mathbf{k}_2)) =$$

$$= \sum_{\mathbf{k}_2} f(\mathbf{k}_2) \sum_{\mathbf{k}_1'} \frac{2\pi}{\hbar} |M|^2(q, q') \delta(\varepsilon(\mathbf{k}_1') + \varepsilon(\mathbf{k}_1 + \mathbf{k}_2 - \mathbf{k}_1') - \varepsilon(\mathbf{k}_1) - \varepsilon(\mathbf{k}_2)).$$

and by homogenization [27] we have

$$\lambda_{ee}(\mathbf{k}_1) \approx \frac{1}{(2\pi)^4} \int_{\mathbb{R}^2} \left[f(\mathbf{k}_2) \int_{\mathbb{R}^2} \frac{2\pi}{\hbar^2 v_F} |M|^2(q, q') \delta(|\mathbf{k}_1'| + |\mathbf{k}_1 + \mathbf{k}_2 - \mathbf{k}_1'| - |\mathbf{k}_1| - |\mathbf{k}_2|)\, \mathrm{d}\mathbf{k}_1' \right] \mathrm{d}\mathbf{k}_2.$$

In the wave-vector $\hbar\mathbf{k}$ space let us consider a mesh made of $N \times N$ square cells of edge $\Delta_{\hbar\mathbf{k}}$. If we characterize each cell by a couple of integers (i, j) and denote by f_{ij} the mean value of $f(\mathbf{k}_2)$ in the cell, one can use the middle point approximation

$$\lambda_{ee}(\mathbf{k}_1) \approx \frac{1}{(2\pi)^3 \hbar^2 v_F} \sum_{i,j=1}^{N} f_{ij} \frac{\Delta_{\hbar\mathbf{k}}^2}{\hbar^2} \left[\int_{\mathbb{R}^2} |M|^2(q, q') \delta(|\mathbf{k}_1'| + |\mathbf{k}_1 + \mathbf{k}_2 - \mathbf{k}_1'| - |\mathbf{k}_1| - |\mathbf{k}_2|)\, \mathrm{d}\mathbf{k}_1' \right] =$$

$$= \frac{\Delta_{\hbar\mathbf{k}}^2}{(2\pi)^3 \hbar^4 v_F} \sum_{i,j=1}^{N} f_{ij} \int_{\Gamma} |M|^2(q, q')\, \mathrm{d}\Gamma.$$

To complete the evaluation we need a parametric representation of Γ.

Let us consider an electron having wave-vector $\mathbf{k}_1$ and associated with it a companion electron having wave-vector $\mathbf{k}_2$. Besides the initial reference frame $\vec{k}_x O \vec{k}_y$, let us consider the reference frame $\vec{k}_x' F_1 \vec{k}_y'$, where F_1 is one of the two foci, $\vec{k}_x' \parallel \mathbf{k}_1 + \mathbf{k}_2$ and $\vec{k}_y' \perp \vec{k}_x'$. Without loss of generality we can choose $O \equiv F_1 \equiv K$ with K Dirac point (see Fig. 1). Let us denote by θ the angle between $\vec{k}_x'$ and $\vec{k}_x$.

Given a point P belonging to the ellipses, let us denote by β the angle between $P - O'$ the $\vec{k}_x'$-axes (see Fig. 1), O' being the center of the ellipses.

The parametric equations of the Γ are

$$\Gamma : \begin{cases} \vec{k}_x = \dfrac{(\mathbf{k}_1 + \mathbf{k}_2)_x}{2} + a \cos\beta \cos\theta - b \sin\beta \sin\theta \\[2mm] \vec{k}_y = \dfrac{(\mathbf{k}_1 + \mathbf{k}_2)_y}{2} + a \cos\beta \sin\theta + b \sin\beta \cos\theta \end{cases}, \qquad \beta \in [0, 2\pi[.$$

and

$$\mathrm{d}\Gamma = \sqrt{\left(\frac{\mathrm{d}\vec{k}_x}{\mathrm{d}\beta}\right)^2 + \left(\frac{\mathrm{d}\vec{k}_y}{\mathrm{d}\beta}\right)^2}\, d\beta = \sqrt{a^2 \sin^2\beta + b^2 \cos^2\beta}\, d\beta.$$
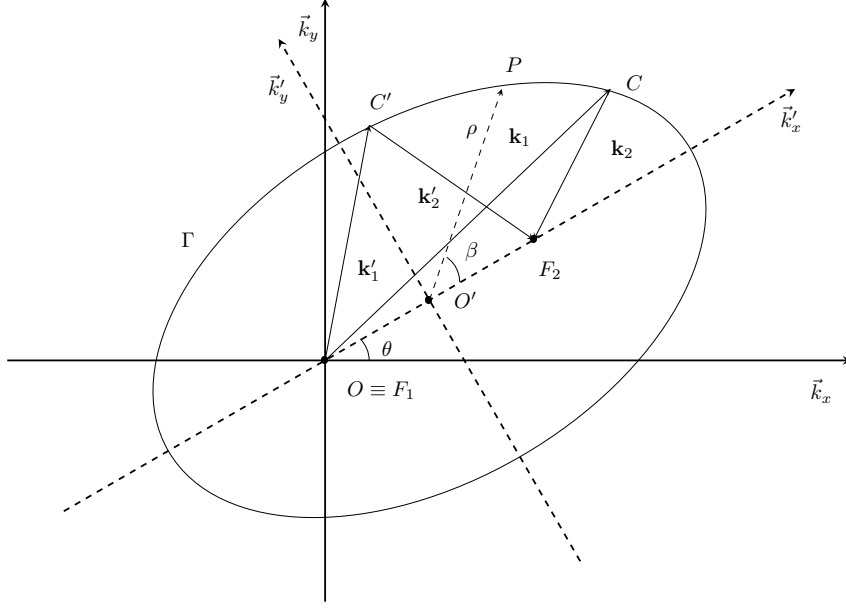
Figure 1: Schematic representation of the electron states before and after the scattering in the original and elliptic reference frames.

The post collision vectors $\mathbf{k}_1'$ and $\mathbf{k}_2'$ are given by

$$\mathbf{k}_1' = C' - F_1 = \left(\frac{(\mathbf{k}_1 + \mathbf{k}_2)_x}{2} + a\cos\beta\cos\theta - b\sin\beta\sin\theta, \frac{(\mathbf{k}_1 + \mathbf{k}_2)_y}{2} + a\cos\beta\sin\theta + b\sin\beta\cos\theta \right),$$

$$\mathbf{k}_2' = F_2 - C' = \left(\frac{(\mathbf{k}_1 + \mathbf{k}_2)_x}{2} - a\cos\beta\cos\theta + b\sin\beta\sin\theta, \frac{(\mathbf{k}_1 + \mathbf{k}_2)_y}{2} - a\cos\beta\sin\theta - b\sin\beta\cos\theta \right).$$

Therefore, the electron-electron scattering rate can be evaluated as

$$\lambda_{ee} \approx \frac{\Delta_{\hbar\mathbf{k}}^2}{(2\pi)^3\hbar^4 v_F} \sum_{i,j=1}^N f_{ij} \int_\Gamma |M|^2(q,q') \, \mathrm{d}\Gamma =$$

$$= \frac{\Delta_{\hbar\mathbf{k}}^2}{(2\pi)^3\hbar^4 v_F} \sum_{i,j=1}^N f_{ij} \int_0^{2\pi} |M|^2(q(\beta),q'(\beta)) \sqrt{a^2\sin^2\beta + b^2\cos^2\beta} \, \mathrm{d}\beta,$$

where

$$q(\beta) = |\mathbf{k}_1 - \mathbf{k}_1'|, \quad q'(\beta) = |\mathbf{k}_1 - \mathbf{k}_2'|.$$

Introducing an uniform mesh of $[0, 2\pi]$ of size $\Delta\beta = 2\pi/m$, $0 = \beta_0 < \beta_1 < \ldots < \beta_k < \beta_{k+1} < \ldots < \beta_m = 2\pi$, and applying the trapezoidal rule, one gets

$$\lambda_{ee} \approx \frac{\Delta_{\hbar\mathbf{k}}^2}{(2\pi)^3\hbar^4 v_F} \sum_{i,j=1}^N f_{ij} \frac{\Delta\beta}{2} \sum_{k=1}^m \left[g(\beta_{k-1}) + g(\beta_k) \right] \quad = C_{ee} \sum_{i,j=1}^N f_{ij} \sum_{k=1}^m \left[\widetilde{g}(\beta_{k-1}) + \widetilde{g}(\beta_k) \right],$$

13

where

$$C_{ee} = \frac{r_s^2 \kappa^2 v_F g_s g_v \Delta_{\hbar\mathbf{k}}^2 \Delta\beta}{512\pi\hbar^2}$$

$$\widetilde{g}(\beta_k) = |\widetilde{M}|^2(q(\beta_k), q'(\beta_k))\sqrt{a^2\sin^2\beta_k + b^2\cos^2\beta_k}, \quad |\widetilde{M}|^2(q(\beta_k), q'(\beta_k))$$

$$= |\widetilde{V}(q(\beta_k))|^2 + |\widetilde{V}(q'(\beta_k))|^2 - \widetilde{V}(q(\beta_k))\widetilde{V}(q'(\beta_k)),$$

$$\widetilde{V}(q(\beta_k)) = \frac{1}{\epsilon(q(\beta_k))q(\beta_k)}\left(1 + \cos(\phi_{\mathbf{k}_1,\mathbf{k}_1'})\right)\left(1 + \cos(\phi_{\mathbf{k}_2,\mathbf{k}_2'})\right),$$

$$\widetilde{V}(q'(\beta_k)) = \frac{1}{\epsilon(q'(\beta_k))q'(\beta_k)}\left(1 + \cos(\phi_{\mathbf{k}_1,\mathbf{k}_2'})\right)\left(1 + \cos(\phi_{\mathbf{k}_2,\mathbf{k}_1'})\right),$$

$$\epsilon(q(\beta_k))q(\beta_k) = q(\beta_k) + C_\epsilon\widetilde{\Pi}(q(\beta_k)),$$

with

$$C_\epsilon = \frac{r_s k_F}{2}(g_s g_v)^{3/2}, \tag{30}$$

$$\widetilde{\Pi}(q(\beta_k)) = \begin{cases} 1 & \text{if} \quad q(\beta_k) < 2k_F \\ 1 + \dfrac{\pi q(\beta_k)}{8k_F} - \dfrac{\sqrt{q^2(\beta_k) - 4k_F^2}}{2q(\beta_k)} - \dfrac{q(\beta_k)}{4k_F}\arcsin\left(\dfrac{2k_F}{q(\beta_k)}\right) & \text{otherwise} \end{cases}$$

$k_F = \sqrt{4\pi n/g_v g_s}$, n being the electron density.

Once a numerical approximation of the transition rate has been obtained, the Monte Carlo simulation proceeds in a standard way. If the electron-electron scattering is selected after a free fly, to the wave-vector $\mathbf{k}_1$ of the considered electron, a companion electron is associated according to the discrete estimation f_{ij} of f at the current time. This is equivalent selecting with a uniform distribution one of the simulated particles, of course apart from the first one. Let $\mathbf{k}_2$ be the wave-vector of the companion electron. With the procedure delineated above one determines the ellipses and randomly chooses the angle $\beta \in [0, 2\pi]$ selecting the point P and, therefore, the wave-vector of the outgoing electrons $\mathbf{k}_1'$ and $\mathbf{k}_2'$. Eventually, in order to take into account the Pauli exclusion principle, one generates two random number $\eta_1, \eta_2 \in [0, 1]$. If $f(\mathbf{k}_1') < \eta_1$ and $f(\mathbf{k}_2') < \eta_2$ the transition is accepted and $\mathbf{k}_1$ and $\mathbf{k}_2$ become $\mathbf{k}_1'$ and $\mathbf{k}_2'$, otherwise the initial states remain unchanged.

5 Bipolar model

As shown in [10], the only allowed interband electron-electron scattering is when the two electrons are initially in different bands and the final states remain in different bands. In particular, carrier multiplication, that is a transition which creates an excess of charge in the conduction band, and Auger recombination, which decreases the charge in the conduction band, are transitions having zero measure in the phase space.

To fix the ideas, without loss of generality let us suppose that $\mathbf{k}_1$ is in the conduction band (CB) while $\mathbf{k}_2$ is in the valence band (VB) and $\mathbf{k}_1'$ is in CB and $\mathbf{k}_2'$ is in VB.

Momentum and energy conservations now lead to the relations

$$\mathbf{k}_1 + \mathbf{k}_2 = \mathbf{k}_1' + \mathbf{k}_2',$$

$$|\mathbf{k}_1| - |\mathbf{k}_2| = |\mathbf{k}_1'| - |\mathbf{k}_2'|.$$

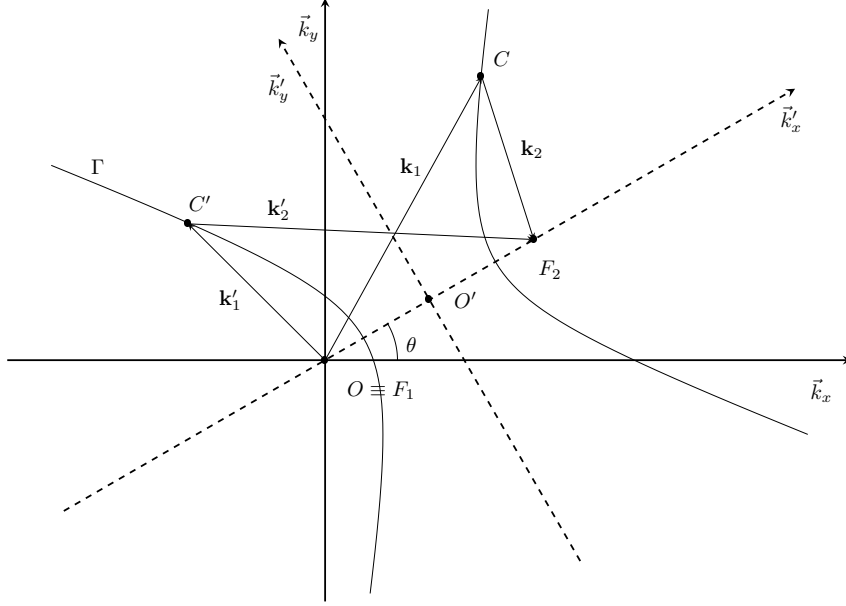which determine a hyperbola $\tilde{\Gamma}$ with distance between foci $2c$ equal to $|\mathbf{k}_1 + \mathbf{k}_2|$.

Figure 2: Schematic representation of the hyperbola arising in an electron-electron scattering rate in the interband case.

If we denote by a the length of the major semi-axis, one has

$$||\mathbf{k}_1| - |\mathbf{k}_2|| = 2a.$$

and from the relation $c^2 = a^2 + b^2$ one gets the length b of the minor semi-axis. The electron-electron scattering rate in the interband case reads

$$\lambda_{ee} = \sum_{\mathbf{k}_2} f(\mathbf{k}_2) \sum_{\mathbf{k}_1'} \frac{2\pi}{\hbar} |M|^2(q, q') \delta(\varepsilon(\mathbf{k}_1') + \varepsilon(\mathbf{k}_1 + \mathbf{k}_2 - \mathbf{k}_1') - \varepsilon(\mathbf{k}_1) - \varepsilon(\mathbf{k}_2))$$

and by homogenization [27], one has

$$\lambda_{ee} \approx \frac{1}{(2\pi)^3} \int_{\mathbb{R}^2} \left[f(\mathbf{k}_2) \int_{\mathbb{R}^2} \frac{1}{\hbar^2 v_F} |M|^2(q, q') \delta(|\mathbf{k}_1'| - |\mathbf{k}_1 + \mathbf{k}_2 - \mathbf{k}_1'| - |\mathbf{k}_1| + |\mathbf{k}_2|) \, \mathrm{d}\mathbf{k}_1' \right] \mathrm{d}\mathbf{k}_2.$$

15

If we discretize the wave-vector space as in the intraband case and denote by f_{ij} the average of $f(\mathbf{k}_2)$ in the cell determined by the indices (i,j), one gets

$$\lambda_{ee} \approx \frac{1}{(2\pi)^3 \hbar^2 v_F} \sum_{i,j=1}^{N} f_{ij} \frac{\Delta_{\hbar\mathbf{k}}^2}{\hbar^2} \left[\int_{\mathbb{R}^2} |M|^2(q,q') \delta(|\mathbf{k}_1'| - |\mathbf{k}_1 + \mathbf{k}_2 - \mathbf{k}_1'| - |\mathbf{k}_1| + |\mathbf{k}_2|) \, d\mathbf{k}_1' \right] =$$

$$= \frac{\Delta_{\hbar\mathbf{k}}^2}{(2\pi)^3 \hbar^4 v_F} \sum_{i,j=1}^{N} f_{ij} \int_{\hat{\Gamma}} |M|^2(q,q') \, d\hat{\Gamma}.$$

To complete the evaluation we need a parametric representation of $\hat{\Gamma}$.

Without loss of generality, we can assume that the foci of the hyperbola have coordinates

$$F_1 = (0,0), \qquad F_2 = ((\mathbf{k}_1 + \mathbf{k}_2)_x, (\mathbf{k}_1 + \mathbf{k}_2)_y).$$

The center is given by

$$O' = \left(\frac{(\mathbf{k}_1 + \mathbf{k}_2)_x}{2}, \frac{(\mathbf{k}_1 + \mathbf{k}_2)_y}{2} \right).$$

A new reference frame, said *hyperbolic*, appears (see Fig. 2). It is centered in O' and has axes such that $\vec{k}_x' \parallel \mathbf{k}_1 + \mathbf{k}_2$ e $\vec{k}_y' \perp \vec{k}_x'$. We denote by θ the angle between the axes $\vec{k}_x'$ and $\vec{k}_x$.

In the hyperbolic reference frame, a parametric representation of $\hat{\Gamma}$ reads

$$\Gamma_1 : \begin{cases} \vec{k}_x' = a \cosh\beta \\ \vec{k}_y' = b \sinh\beta \end{cases}, \quad \beta \in \mathbb{R}; \qquad \Gamma_2 : \begin{cases} \vec{k}_x' = -a \cosh\beta \\ \vec{k}_y' = b \sinh\beta \end{cases}, \quad \beta \in \mathbb{R},$$

where Γ_1 and Γ_2 represent the two branches of the hyperbola. Therefore

$$\lambda_{ee} = \frac{\Delta_{\hbar\mathbf{k}}^2}{(2\pi)^3 \hbar^4 v_F} \sum_{i,j=1}^{N} f_{ij} \left[\int_{\Gamma_1} |M|^2(q,q') \, d\Gamma_1 + \int_{\Gamma_2} |M|^2(q,q') \, d\Gamma_2 \right]. \qquad (31)$$

with

$$d\Gamma_i = \sqrt{a^2 \sinh^2\beta + b^2 \cosh^2\beta} \, d\beta, \quad i = 1, 2.$$

At variance with the intraband case, now the evaluation of λ_{ee} requires an integration on a curve which is not limited. However, as observed in [23] we expect that the electron distribution can be considered negligible outside a compact set Ω in the wave-vector space and in the simulation the integral in (31) will be performed over $\hat{\Gamma} \cap \Omega$.

6 Simulations in suspended monolayer graphene

As first step, we are interested in studying how the transport properties are influenced by the electron-electron scattering in a homogeneous suspended monolayer of graphene. To

this aim, we look for spatially homogeneous solutions with a constant electric field with different values of the Fermi energy.

One can control the shift of the Fermi energy ε_F from the Dirac point by a suitable gate voltage (see Fig. 3), creating a kind of n-doping (if $\varepsilon_F > 0$) or p-doping (if $\varepsilon_F < 0$). If the absolute value of the Fermi energy is more than about 0.15 eV, the interband scattering becomes negligible on account of the Pauli exclusion principle, and a unipolar simulation is enough. For lower values a full interband simulation must be performed.

In the following we consider Fermi energies such that a unipolar situation is physically justified. The Boltzmann equation in a single valley reads

$$\frac{\partial f(\mathrm{t}, \mathbf{k})}{\partial t} - \frac{e}{\hbar} \mathbf{E} \cdot \nabla_{\mathbf{k}} f(\mathrm{t}, \mathbf{k}) = C[f], \tag{32}$$

which remains an integral-differential equations, 2D in the wave-vector space.

As initial condition we take the Fermi-Dirac distribution

$$f(0, \mathbf{k}) = \frac{1}{1 + \exp\left(\dfrac{\varepsilon(\mathbf{k}) - \varepsilon_F}{k_B T}\right)},$$

with T room temperature (300 K). Fermi energy is related to the charge density, which remains constant in the unipolar case, by

$$\rho(t) = \rho(0) = \frac{g_s g_v}{(2\pi)^2} \int f(0, \mathbf{k}) \, d\mathbf{k}, \tag{33}$$

where $g_s = 2$ and $g_v = 2$ are the spin and valley degeneracies, respectively.

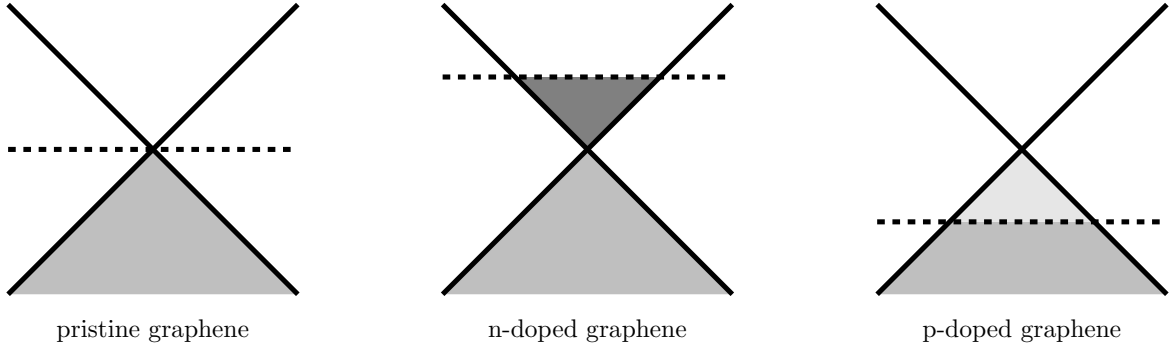|		
pristine graphene	n-doped graphene	p-doped graphene

Figure 3: Shift of the Fermi energy (dashed line) with respect to the Dirac point (vertex of the cone).

All the electron-phonon scatterings have been included as in [13, 28, 26, 29, 4]. The numerical simulations with different values of the Fermi energy (and as consequence the electron density) in a range where the unipolar description is justified. We used the Direct

Simulation Monte Carlo devised in [13] by adding the electron-electron scattering. At variance with the electron-phonon scattering, for the electron-electron scattering we need to update the scattering rate after each collision event due to the presence of the electron distribution. This, of course, increases hugely the computing time. $N_p = 2 \cdot 10^4$ particles have been used. As an alternative hydrodynamical models can be formulated (the interested read is referred to [30, 31, 32, 33, 34]).

In Fig.s 4 the steady distribution functions at Fermi level 0.15 eV (top) and 0.25 eV (bottom) are shown in the case of applied electric fields 1kV/cm (left), 3kV/cm (right). Note that the distributions never exceed one and, therefore, no violation of the Pauli exclusion principle is observed.
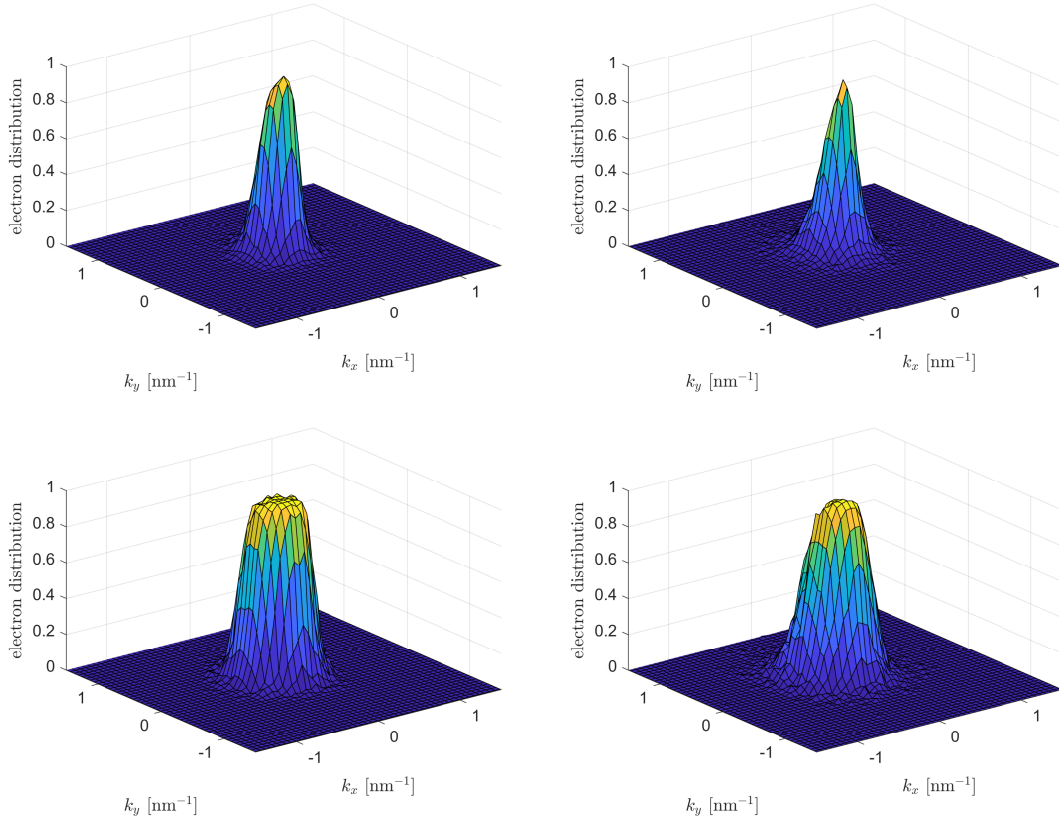

Figure 4: Steady distribution functions at Fermi level 0.15 eV (top) and 0.25 eV (bottom) with applied electric fields 1kV/cm (left), 3kV/cm (right).

In Fig.s 5, 6 the mean velocity $V(t)$ and mean energy $W(t)$, defined as

$$V(t) = \frac{1}{\rho(t)} \frac{g_s g_v}{(2\pi)^2} \int \mathbf{v} f(t, \mathbf{k}) \, d\mathbf{k}, \quad W(t) = \frac{1}{\rho(t)} \frac{g_s g_v}{(2\pi)^2} \int \mathbf{v} f(t, \mathbf{k}) \, d\mathbf{k}, \qquad (34)$$

are shown versus time with and without the electron-electron scattering. As appears from the plots, the electron-electron scattering makes the mean velocity lower. The difference
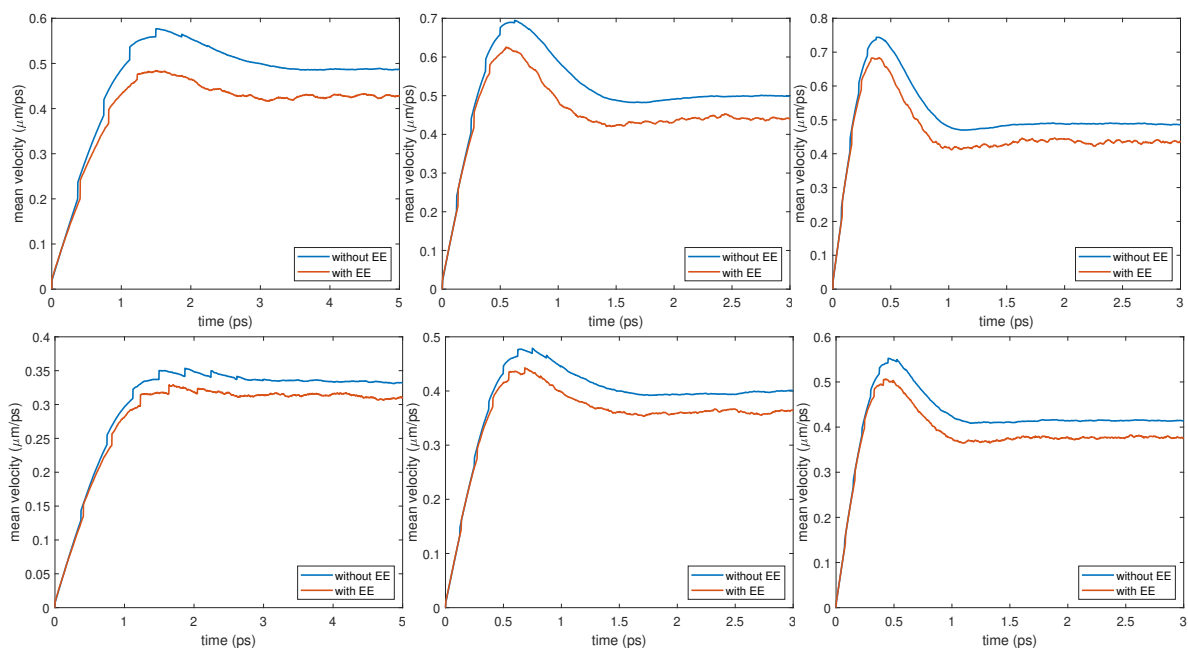
Figure 5: Mean velocity versus time at Fermi level 0.15 eV (top) and 0.25 eV (bottom) with applied electric fields 1kV/cm (left), 3kV/cm (center), 5kV/cm (right).

in the velocity is about 13% both when $\varepsilon_F = 0.15$ eV and $\varepsilon_F = 0.25$ eV. Apparently, a degradation of the velocity could seem in contrast with the property of momentum conservation. However, the group velocity is not proportional to the crystal momentum, as happens in the parabolic band structure, and momentum conservation does not imply velocity conservation. Of course a reduction of the mean velocity implies a non negligible degradation of then current. Moreover, the differences in the velocities influence also the balance equation for the energy. Therefore, despite the property of the electron-electron collision operator of conserving the energy, indeed an effective degradation of the average energy is obtained. Our results are in qualitative agreement with those reported in [5] where a standard Monte Carlo approach has been adopted.

Conclusion and acknowledgments

The main analytical properties of the electron-electron scattering have been investigated, in particular the collisional invariants and the equilibria which are more general than the Fermi-Dirac distribution. The scattering rate has been evaluated and used in DSMCs. The obtained results highlight the importance of the electron-electron scattering for the correct determination of the currents and, therefore, of the characteristic curves.

As future improvements, the dynamics of phonons could be added, e.g. by using the approaches in [14, 28, 35, 36] and some quantum corrections added and simulated for example as in [37].

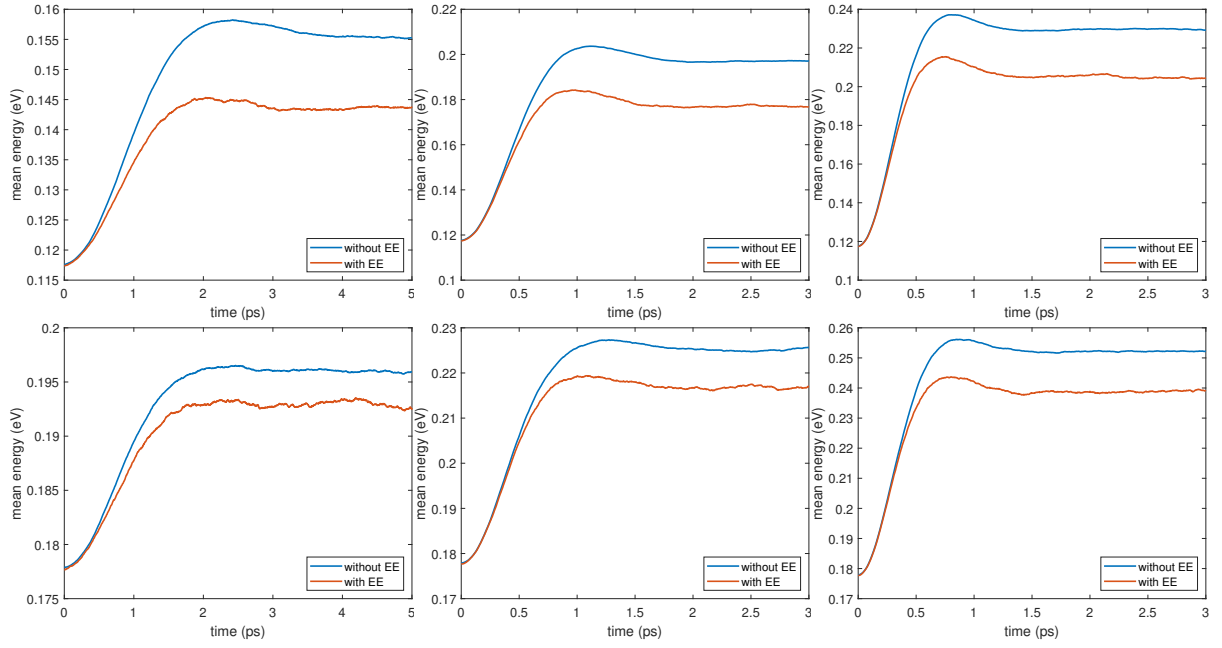The authors thank Prof. A. Majorana for the stimulating discussions.

Figure 6: Mean energy versus time at Fermi level 0.15 eV (top) and 0.25 eV (bottom) with applied electric fields 1kV/cm (left), 3kV/cm (center), 5kV/cm (right).

References

[1] V. N. Kotov, B. Uchoa, V. M. Pereira, F. Guinea, and A. H. Castro Neto, *Electron-Electron Interactions in Graphene: Current Status and Perspectives*, Rev. Mod. Phys., 84, 1067 (2012). doi: 10.1103/RevModPhys.84.1067.

[2] A. Tomadin, D. Brida, G. Cerullo, A. C. Ferrari, and M. Polini, *Nonequilibrium dynamics of photoexcited electrons in graphene: Collinear scattering, Auger processes, and the impact of screening*, Phys. Rev. B, 88, 035430 (2013). doi: 10.1103/PhysRevB.88.035430.

[3] X. Li, E. A. Barry, J. M. Zavada, M. Buongiorno Nardelli, and K. W. Kim, *Influence of electron-electron scattering on transport characteristics in monolayer graphene*, App. Phys. Lett., 97, 082101 (2010). doi: 10.1063/1.3483612.

[4] M. V. Fischetti, J. Kim, S. Narayanan, Z.-Y. Ong, C. Sachs, D. K. Ferry, S. J. Aboud, *Pseudopotential-based studies of electron transport in graphene and graphene nanoribbons*, J. Phys. Cond. Mat., 25, 473202 (2013). doi: 10.1088/0953-8984/25/47/473202.

[5] T. Fang, A. Konar, H. Xing, and D. Jena, *High-field transport in two-dimensional graphene*, Phys. Rev. B, 84, 125450 (2011). doi: 10.1103/PhysRevB.84.125450.

[6] E. Sano, *Monte Carlo Simulation of Ultrafast Electron Relaxation in Graphene*, App. Phys. Expr., 4, 085101 (2011). doi: 10.1143/APEX.4.085101.

[7] P. Borowik, J. L. Thobel, and L. Adamowicz, *Modified Monte Carlo method for study of electron transport in degenerate electron gas in the presence of electron-electron interactions, application to graphene*, J. Comput. Phys., 341, 397–405 (2017). doi: 10.1016/j.jcp.2017.04.011.

[8] E. H. Hwang, and S. Das Sarma. *Dielectric function, screening, and plasmons in two-dimensional graphene*, Phys. Rev. B, 75, 205418 (2007). doi: 10.1103/PhysRevB.75.205418.

[9] S. Das Sarma, S. Adam, E. H. Hwang, and E. Rossi, *Electronic transport in two-dimensional graphene*, Rev. Mod. Phys., 83, 407 (2011). doi: 10.1103/RevModPhys.83.407.

[10] D. Brida, A. Tomadin, C. Manzoni, Y.J. Kim, A. Lombardo, S. Milana, R.R. Nair, K.S. Novoselov, A.C. Ferrari, G. Cerullo, and M. Polini, *Ultrafast collinear scattering and carrier multiplication in graphene*, Nat. Comm., 4, 1987 (2013). doi: 10.1038/ncomms2987.

[11] C. Cercignani, and G. M. Kremer, *The Relativistic Boltzmann Equation: Theory and Application*, Birkhäuser Basel, 2002.

[12] A. Shytov, M. Rudner, N. Gu, M. Katnelson, and L. Levitov, *Atomic collapse, Lorentz boosts, Klein scattering, and other quantum-relativistc phenomena in graphene*, Solid State Commun., 149, 1087–1093 (2009). doi: 10.1016/j.ssc.2009.02.043.

[13] V. Romano, A. Majorana, and M. Coco, *DSMC method consistent with the Pauli exclusion principle and comparison with deterministic solutions for charge transport in graphene*, J. Comput. Phys., 302, 267–284 (2015). doi: 10.1016/j.jcp.2015.08.047.

[14] M. Coco, and V. Romano, *Simulation of Electron-Phonon Coupling and Heating Dynamics in Suspended Monolayer Graphene Including All the Phonon Branches*, J. Heat Transfer, 140, 092404 (2018). doi: 10.1115/1.4040082.

[15] O. Morandi, P.-A. Hervieux, G. Manfredi, *Bose-Einstein condensation of positronium: Modification of the s-wave scattering length below to the critical temperature*, J. Phys. B: At. Mol. Opt. Phys., 49, 084002 (2016). doi: 10.1088/0953-4075/49/8/084002.

[16] O. Morandi, P.-A. Hervieux, G. Manfredi, Bose-Einstein-condensation dynamics with a quantum-kinetic approach, Phys. Rev. A, 88, 023618 (2013). doi: 10.1103/PhysRevA.88.023618.

[17] P. R. Wallace, *The band theory of graphite*, Phys. Rev., 71, 662 (1947). doi: 10.1103/PhysRev.71.622.

[18] C. Cercignani, *The Boltzmann Equation and Its Applications*, Springer, New York, 1988.

[19] N. Ben Abdallah, and P. Degond, *On a hierarchy of macroscopic models for semiconductors*, J. Math. Phys., 37, 3306 (1996). doi: 10.1063/1.531567.

[20] A. Jüengel, *Transport equations for semiconductors*, Springer Berlin, Heidelberg, 2009.

[21] A. Majorana, *Equilibrium solutions of the non-linear Boltzmann equation for an electron gas in a semiconductors*, Il Nuovo Cimento B, 108, 871–877 (1993). doi: 10.1007/BF02828734.

[22] P. Lichtenberger, O. Morandi, and F. Schürrer, *High-field transport and optical phonon scattering in graphene*, Phys. Rev. B 84, 045406 (2011). doi: 10.1103/PhysRevB.84.045406.

[23] G. Nastasi, V. D. Camiola, and V. Romano, *Direct Simulation of Charge Transport in Graphene Nanoribbons*, Commun. Comput. Phys., 31, 449–494 (2022). doi: 10.4208/cicp.OA-2021-0032.

[24] I. Wadgaonkar, R.Jain, and M.Battiato, *Numerical scheme for the far-out-of-equilibrium time-dependent Boltzmann collision operator: 1D second-degree momentum discretisation and adaptive time stepping*, Comput. Phys. Commun., 263, 107863 (2021). doi: 10.1016/j.cpc.2021.107863.

[25] I. Wadgaonkar, M. Waisab, and M. Battiato, *Numerical solver for the out-of-equilibrium time dependent Boltzmann collision operator: Application to 2D materials*, Comput. Phys. Commun., 271, 108207 (2022). doi: 10.1016/j.cpc.2021.108207.

[26] M. Coco, A. Majorana, and V. Romano, *Cross validation of discontinuous Galerkin method and Monte Carlo simulations of charge transport in graphene on substrate*, Ricerche Mat., 66, 201–220 (2016). doi: 10.1007/s11587-016-0298-4.

[27] C. Jacoboni, *Theory of Electron Transport in Semiconductors*, Springer Berlin, Heidelberg, 2010.

[28] M. Coco, G. Mascali, and V. Romano, *Monte Carlo analysis of thermal effects in monolayer graphene*, J. Comput. Theor. Transp., 45, 540–543 (2016). doi: 10.1080/23324309.2016.1211537.

[29] M. Coco, P. Bordone, L. Demeio, and V. Romano, *Pauli principle and the Monte Carlo method for charge transport in graphene*, Phys. Rev. B, 104, 205410 (2021). doi: 10.1103/PhysRevB.104.205410.

[30] L. Barletti, *Hydrodynamic equations for electrons in graphene obtained from the maximum entropy principle*, J. Math. Phys. 55, 083303 (2014). doi: 10.1063/1.4886698.

[31] O. Morandi, L. Barletti, *Particle Dynamics in Graphene: Collimated Beam Limit*, J. Comput. Theor. Transp., 43, 418–432 (2014). doi: 10.1080/00411450.2014.942917.

[32] L. Luca, G. Mascali, G. Nastasi, V. Romano, *Comparing kinetic and MEP model of charge transport in graphene*, J. Comput. Theor. Transp., 49, 368–388 (2020). doi: 10.1080/23324309.2020.1822870.

[33] L. Luca, V. Romano, *Comparing linear and nonlinear hydrodynamical models for charge transport in graphene based on the Maximum Entropy Principle*, Int. J. Non Linear Mech., 104, 39–58 (2018). doi: 10.1016/j.ijnonlinmec.2018.01.010.

[34] L. Luca, V. Romano, *Quantum corrected hydrodynamic models for charge transport in graphene*, Ann. of Phys., 406, 30–53 (2019). doi: 10.1016/j.aop.2019.03.018.

[35] G. Mascali, V. Romano, *A hierarchy of macroscopic models for phonon transport in graphene*, Physica A, 548, 124489 (2020). doi: 10.1016/j.physa.2020.124489.

[36] G. Mascali, *Exploitation of the Maximum Entropy Principle in the Study of Thermal Conductivity of Silicon, Germanium and Graphene*, Energies, 15, 4718 (2022). doi: 10.3390/en15134718.

[37] O. Muscato, W. Wagner, *A Class of Stochastic Algorithms for the Wigner Equation*, SIAM J. Sci. Comput., 38, A1483–A1507 (2016). doi: 10.1137/16M105798X.